

## A Model for Diagnosing the Formation of Internal Cracks in Continuously Cast Slabs

Zhiqiang Han<sup>1</sup>, Weixia Yuan<sup>2</sup>, Kaike Cai<sup>1</sup>

1) Metallurgy School, University of Science and Technology Beijing, Beijing 100083, China

2) Wuhan Iron and Steel Co., Wuhan 430080, China

(Received 1999-05-25)

**Abstract:** The internal cracks in continuously cast slabs are attributed to the excessive tensile strain occurring at the solidifying front during the continuous casting process. Based on the understanding, a model for diagnosing the formation of the internal cracks was established, in which the strains at the solidifying front caused by bulging, straightening or unbending, and roll misalignment were calculated and compared with a critical strain value to estimate whether the internal cracks form. Moreover, the established model was applied to a real slab caster to reveal the distribution of the strains in casting direction and its effect on the internal cracks. It was proved that the model was reliable and useful for optimizing the operation of continuous casting.

**Key words:** continuous casting; slab; internal crack; diagnosis; model

Internal cracks are a type of defect frequently occurring in continuously cast slabs, and it is usually accompanied by serious segregation and is harmful to the uniformity and continuity of steel. It has been proved that internal cracks are caused by the excessive tensile strain originating at the solidifying front. During continuous casting, the segregation of sulfur near solidifying interface leads to the formation of sulfide film around columnar crystals. The sulfide film has low melting point and decreases the ability of the solidifying front against deformation. At the same time, the solidifying front is continuously under the action of the strains resulting from bulging, straightening or unbending, and roll misalignment. Once these strains exceed a critical value, the solidifying front would crack along the boundaries of the columnar crystals and internal cracks would be formed. Therefore, the key to prevent the formation of internal cracks is to control the tensile strain at the solidifying front under the critical strain level.

In order to calculate the strains at the solidifying front, some researchers developed the finite element model on bulging [1], roll misalignment [2], unbending [3], and thermal strain [4]. But these models were just studies in laboratory and can not be applied in real production because of the complexity of finite element analysis and the lack of constitutive relationship describing the mechanical behavior of steel at elevated temperature.

Based on a model of heat transfer and solidification for continuously cast slabs, this paper presented a model

for analyzing the tensile strains at solidifying front and diagnosing the formation of internal cracks by using empirical equations of strain analysis. Moreover, this model was applied to a real slab caster to study the distribution of the strains mentioned above along the length of the slab and to investigate the relationship between internal cracks and the strains.

### 1 Model Description

#### 1.1 Model for heat transfer and solidification

According to the characteristics of heat transfer and solidification of continuously cast slabs, a quarter of slab section was taken as the calculation domain. The heat transfer and solidification of the domain during its movement through the mold, secondary cooling zone, and air cooling zone were governed by the following 2-dimensional transient heat conduction equation,

$$\rho c \frac{\partial T}{\partial t} = \frac{\partial}{\partial x} \left( \lambda \frac{\partial T}{\partial x} \right) + \frac{\partial}{\partial y} \left( \lambda \frac{\partial T}{\partial y} \right) + \rho L \frac{\partial f_s}{\partial t} \quad (1)$$

where  $\rho$ ,  $c$ ,  $\lambda$  are the density, special heat capacity, and heat conductivity of steel respectively;  $L$  is the total latent heat; and  $f_s$  the solid fraction. The equation was solved by finite differential method. The release of the latent heat was treated by the enthalpy method.

By solving the above heat transfer and solidification model, the distribution of surface temperature and the thickness of solidified shell along the length of the slab were obtained and provided to the strain analysis and internal crack diagnosis model as input parameters.

## 1.2 Model for strain analysis and internal crack diagnosis

In the strain analysis and internal crack diagnosis model, the strains at the solidifying front caused by bulging, straightening or unbending, and roll misalignment were calculated by using the output data, the distribution of surface temperature and the thickness of solidified shell in casting direction. In the calculation, the following empirical equations for strain analysis were adopted [2,5,6],

$$\delta_B = \frac{pl^4}{32 E_e S^3} \sqrt{t} \quad (2)$$

$$\varepsilon_B = \frac{1600 S \delta_B}{l^2} \quad (3)$$

$$\varepsilon_S = 100 \times \left( \frac{d}{2} - S \right) \times \left| \frac{1}{R_{n-1}} - \frac{1}{R_n} \right| \quad (4)$$

$$\varepsilon_M = \frac{300 S \delta_M}{l^2} \quad (5)$$

where  $\delta_B$  is the slab bulging amount;  $p$ , the static pressure;  $l$ , the roll pitch;  $E_e$ , the equivalent elastic modulus;  $S$ , the shell thickness;  $t$ , the time for the slab to travel a roll pitch;  $d$ , the slab thickness;  $R_{n-1}$  and  $R_n$ , the unbending radii;  $\delta_M$ , the roll misalignment amount;  $\varepsilon_B$ , the bulging strain;  $\varepsilon_S$ , the straightening strain; and  $\varepsilon_M$ , the misalignment strain.

Providing that these strains can be linearly added up, the total strain at the solidifying front can be calculated as

$$\varepsilon_T = \varepsilon_B + \varepsilon_S + \varepsilon_M \quad (6)$$

## 2 Calculated Results and Discussion

The calculation was based on a fully bowed continuous caster that has 18 segments and 98 pairs of rolls in its secondary cooling zone. The roll diameter and the roll pitch vary from  $\phi 155$  to  $\phi 325$  mm and from 199 to 370 mm respectively. The metallurgical length of the caster is about 33 m. The radius of the caster is 10.5 m. A four-point unbending system is adopted, in which the unbending radii are 13.5, 19.5 and 38.0 m.

### 2.1 Results of heat transfer model and its reliability

The reliability of the heat transfer and solidification model is very important to the strain analysis and internal crack diagnosis model. The results of the heat transfer model were verified by using the measured surface temperature and the data of liquid core length offered by the caster manufacturer. **Figure 1** shows the variation of the surface temperature at the exit of the caster, which was measured by AGA-80SC, a type of infrared instrument made in the Sweden. The average value of the measured temperature data is  $886^\circ\text{C}$ , while the cal-

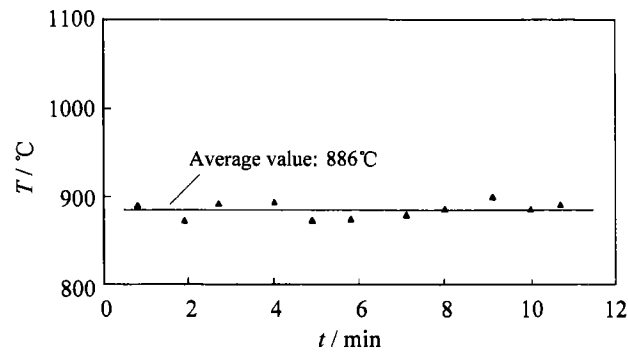


**Figure 1** Measured surface temperature at the exit of the caster. Steel Q235, section size 1 550 mm  $\times$  230 mm, casting speed 1.12 m/min, pouring temperature 1 528–1 537 $^\circ\text{C}$ , and secondary cooling water 0.76 L/kg.

culated surface temperature is  $903^\circ\text{C}$ . The relative error is less than 3%. Additionally, the data of liquid core length offered by the caster manufacturer were used for further verification of the heat transfer model. The results showed that the relative error of the model is usually less than 5%, and the maximum error is no more than 8%. For example, under the conditions of structural steel, section size 1550 mm  $\times$  230 mm, and casting speed 1.0 m/min, the length of liquid core offered by the caster manufacturer is 20.0 m, while the calculated length of the model is 20.7 m. The relative error is 3.5%. It is proved by the above calculation and comparison that the heat transfer model has the ability to provide reliable data for the strain analysis and internal crack diagnosis model.

### 2.2 Distribution of bulging strain along the length

The distribution of bulging strain at the solidifying front along the length of the slab is shown in **figure 2**. It can be seen that from the upper part to the lower part of the caster, the bulging strain first increases gradually

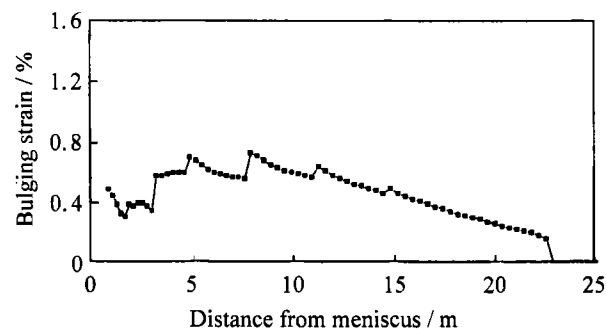


**Figure 2** Distribution of bulging strain in casting direction. Steel Q235, section size 1 550 mm  $\times$  230 mm, casting speed 1.0 m/min.

and then decreases slowly. Although the value of the bulging strain would vary when the operation condition is changed, the distribution of the strain along the length of the slab has nearly the same characteristics. It is known that the bulging between two adjacent rolls mainly depends on the static pressure of liquid steel, the

roll pitch, and the thickness of solidified shell. When the slab just moves out of the mold, although the solidified shell is thin and the surface temperature is high, the slab bulging is not serious because the static pressure is not large enough and the rolls are arranged closely. Correspondingly, the bulging strain at the solidifying front is not very large. With the downward movement of the slab, the static pressure of liquid steel increases significantly and the roll pitch increases to some extent, while the thickness of the solidified shell has not been increased to a certain level at which the shell is strong enough to resist the static pressure. Therefore, obvious bulging takes place. As a result, very serious strain occurs at the solidifying front. In general, the segments where large bulging can easily occur are the most dangerous zones where internal cracks frequently originate.

### 2.3 Straightening strain

The straightening strain only originates in the unbending zone of the caster and occurs as tensile strain at the solidifying front of upper solidified shell of the slab. In general, the straightening strain is about 0.1% and is only 15%–20% of the bulging strain for a multi-point unbending caster, which is shown in **figure 3**.

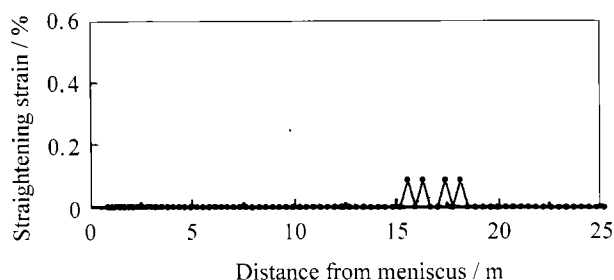


**Figure 3** Distribution of straightening strain in casting direction. Steel Q235, section size 1 550 mm × 230 mm, casting speed 1.0 m/min.

### 2.4 Roll misalignment strain

The deviation and deformation of the supporting rolls can cause additional strain at the solidifying front of the slab. **Figure 4** shows the strain caused at the solidifying front by the assumed amount of roll misalignment, 0.5, 1.0 and 1.5 mm. It is necessarily to be specified that the figure does not represent a real distribution of the misalignment strain. Each datum point in the figure only represents the strain value caused by the corresponding roll when this roll is assumed to be the only roll with a certain amount of misalignment in the whole caster. From the figure it can be seen that the strain at the solidifying front caused by a certain amount of misalignment is higher in the segments with thicker solidified shell than that in the segments with thinner solidified shell. In other words, the harmful effect of roll mis-

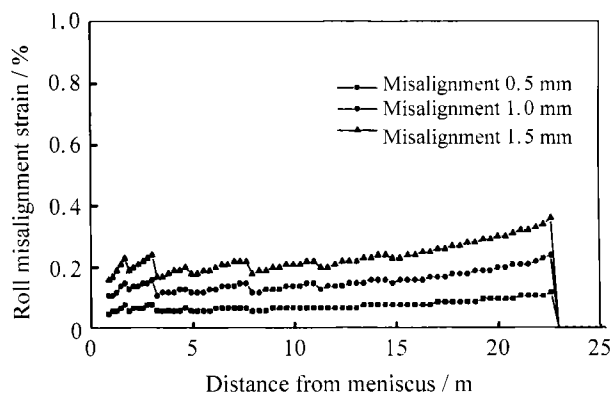


**Figure 4** Misalignment strain under different amount of roll misalignment. Steel Q235, section size 1 550 mm × 230 mm, casting speed 1.0 m/min.

alignment is especially significant in segments where the solidified shell is thick. So, more attention should be paid to the precision of the middle and lower rolls of the caster.

### 2.5 Calculation on a real slab

The formation of internal cracks depends upon the strains at the solidifying front and the critical strain. The relationship between the strains at the solidifying front and the formation of internal cracks was investigated. A half of the section of a slab block sampled from production was examined by sulfur print to reveal the internal cracks in the slab. The section size of the slab is 1 550 mm × 250 mm, the casting speed is 1.15 m/min, and the composition of the steel is 0.19%C, 0.23%Si, 0.45%Mn, 0.018%P, 0.026%S, 0.005%Al, 0.040%Cu and 0.045%Ni in mass fraction. The sulfur print shows that the internal cracks are clearly discernible and almost all the cracks lie in the range of 30–80 mm inside the surface of the slab.

The critical strain is mainly decided by the composition of steel. Hiebler, *et al.* [7] summarized the results of many researchers and gave the relationship between critical strain and steel composition, which is shown in **figure 5**. The carbon equivalent in mass fraction  $w_{C,p}$  can be calculated with the following equation,

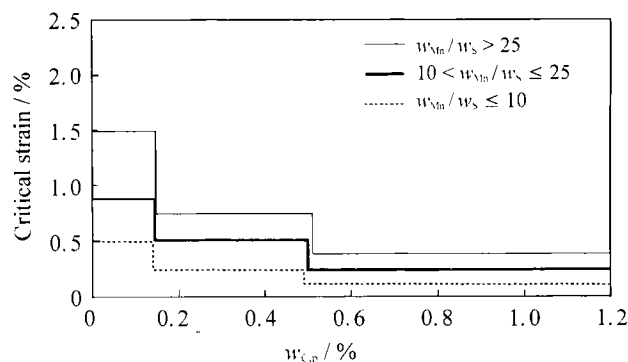


**Figure 5** Relationship of critical strain and steel composition.

$$w_{c,p} = w_c + 0.02w_{Mn} + 0.04w_{Ni} - 0.1w_{Si} - 0.04w_{Cr} - 0.1w_{Mo} \quad (7)$$

where  $w_A$  is the mass fraction of A (A denotes C, Mn, Ni, Si, Cr, Mo, S, etc.). The mass fraction ratio of Mn to S  $w_{Mn}/w_S$  and carbon equivalent  $w_c$  can be calculated from the composition of steel and the critical strain can be determined from figure 5 by using the calculated  $w_{Mn}/w_S$  and  $w_c$ .  $w_{Mn}/w_S$  and  $w_c$  corresponding to the composition of the steel are 17.3 and 0.178 respectively. By using figure 5, it can be determined that the critical strain of the steel is about 0.5%.

The total strain at the solidifying front was calculated by using the developed model. In the calculation, the roll misalignment strain was ignored for the moment because of the lack of roll gap measurement data. In other words, the bulging strain and straightening strain were mainly considered in the calculation. **Figure 6** shows the comparison of the total strain at the solidifying front with the critical strain. From this fig-

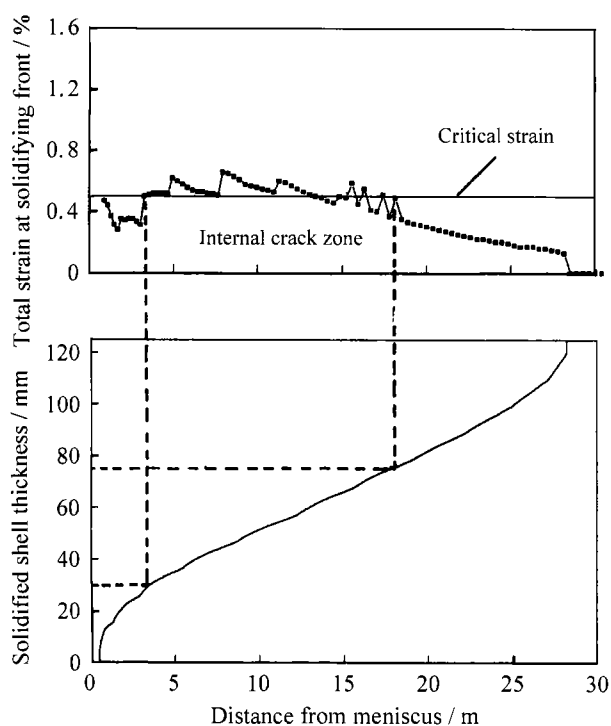


**Figure 6** Corresponding relationship between total strain and internal crack. Steel Q235, section size 1550 mm × 250 mm, casting speed 1.15 m/min.

ure, it can be seen that the range of 3–18 m under the meniscus where the total strain at the solidifying front exceeds the critical value is the range in which internal cracks easily occur. That is to say, this range is susceptible to the internal cracks. According the variation of the thickness of solidified shell along the length of the slab, the susceptible range in the caster just corresponds to the scope of 30–75 mm inside the surface of the slab. This result coincides with that of the sulfur print examination. It proved that the developed model can reflect the real situation of production and is reliable.

### 3 Conclusions

(1) In casting direction, the bulging strain at the solidifying front firstly increases gradually and then decreases slowly. For a bow caster, serious bulging usually occurs in the middle and lower parts of the caster under normal casting speed.

(2) For a caster with multi-point unbending system, the straightening strain at the solidifying front is about 15%–20% of the bulging strain.

(3) Because the harmful effect of roll misalignment is especially significant in the segments where solidified shell thickens, more attentions should be paid to the precision of roll position in such segments.

(4) The reliability of the developed model was verified by sulfur print examination of real slab.

### References

- [1] A. Grill, K. Schwerdtfeger: *Ironmaking and Steelmaking*, 6 (1979), p.131.
- [2] B. Barber, A. Perkins: *Ironmaking and Steelmaking*, 16 (1989), p.406.
- [3] M. Uehara, I. V. Samarasekera, J. K. Brimacombe: *Ironmaking and Steelmaking*, 13(1986), p.138.
- [4] A. Grill, J. K. Brimacombe, F. Weinberg. *Ironmaking and Steelmaking*, 3(1976), p.38.
- [5] Yiping Sheng, Jiquan Sun, Min Zhang: *Iron and Steel* (in Chinese), 28(1993), p.20.
- [6] Guangchou Cao: *Modern Continuous Casting of Slabs* (in Chinese). Metallurgy Industry Press, Beijing, 1994.
- [7] H. Hiebler, J. Zirngast, C. Bernhard, et al.: [in:] *Steelmaking Conference Proceedings*. 1994, p.405.